Energy & Environmental Science

PAPER

View Article Online
View Journal | View Issue



Cite this: *Energy Environ. Sci.*, 2016, **9**, 2654

# Thermophotovoltaics: a potential pathway to high efficiency concentrated solar power†

Hamid Reza Seyf*[a] and Asegun Henry[abc]

A high temperature thermophotovoltaic (TPV) system is modeled and its system level performance is assessed in the context of concentrated solar power (CSP) with thermal energy storage (TES). The model includes the treatment of the emitter and the heat transfer fluid that draws thermal energy from the TES, which then allows for the identification and prioritization of the most important TPV cell/module level properties that should be optimized to achieve maximum performance. The upper limiting efficiency for an idealized system is then calculated, which shows that TPV with TES may one day have the potential to become competitive with combined cycle turbines, but could also offer other advantages that would give CSP an advantage over fossil based alternatives. The system concept is enabled by the usage of liquid metal as a high temperature heat transfer and TES fluid. The system concept combines the great economic advantages of TES with the potential for low cost and high performance derived from TPV cells fabricated on reusable substrates, with a high reflectivity back reflector for photon recycling.

Received 12th May 2016,
Accepted 4th July 2016

DOI: 10.1039/c6ee01372d

www.rsc.org/ees

**Broader context**

Current approaches to concentrated solar power (CSP) rely on the same heat engines as fossil fuels, and thus the only way CSP can become cost competitive is if the cost of collecting and storing high temperature heat from the sun can become less expensive than the heat delivered by fossil fuels. However, the sun is a fundamentally different type of heat source than the sensible heat that can be derived from a fossil fuel. Thus, it would be highly advantageous to pursue systems that can somehow exploit the fundamental advantages of solar energy over fossil fuels towards achieving higher performance and lower cost. This study reports modeling results for such a system, which is based on a thermophotovoltaic (TPV) heat engine instead of a turbine, and the results suggest that TPV has the potential to offer competitive cost and performance.

## Introduction

Thermophotovoltaics (TPV) have been around for decades[1–35] and although there has been interest in using them for solar energy conversion, there has not been a major increase in interest. This has largely been because the efficiency of TPV systems is considered to be low as compared to other options for heat engines. Furthermore, full system level analyses are lacking. Analyses that go beyond the cell/module and actually examine the heat source and how the heat is transferred from the source to the emitter and then into the cell, while also keeping track of all heat losses, are needed. Here, it is also critical to appreciate that one primary metric that has been used to assess TPV cell efficiencies is, what we have termed herein, the full spectrum efficiency (FSE), given by,

$$\eta_{\mathrm{FSE}} = \frac{\dot{W}}{Q_{\mathrm{in}}} \tag{1}$$

where $\dot{W}$ and $Q_{\mathrm{in}}$ are the output work and the total incident light input to the cell, respectively. This metric is useful, particularly because it allows one to compare all cells on equal ground, as authors typically specify that the efficiency was evaluated for a black body emitter at a certain temperature.[36–38] The problem with using the FSE, however, is that the actual value is often low, in the range of 5–20%.[39] This often leads one to believe that the cells are quite inefficient by comparison to other heat engine technologies such as Rankine and Brayton cycles, which typically have efficiencies above 30%. Furthermore, when one considers the high emitter temperatures needed ($>1000$ °C) for TPV to have a competitive power density (*e.g.*, $>10$ kW m$^{-2}$), other options such as a combined cycle, which can have

[a] *George W. Woodruff School of Mechanical Engineering, Georgia Institute of Technology, Atlanta GA, 30332, USA. E-mail: HRS@gatech.edu*
[b] *School of Materials Science and Engineering, Georgia Institute of Technology, Atlanta GA, 30332, USA*
[c] *Heat Lab, Georgia Institute of Technology, Atlanta GA, 30332, USA*

† Electronic supplementary information (ESI) available. See DOI: 10.1039/c6ee01372d

efficiencies as high as 60% and costs below \$2 $W^{-1}$ (here W refers to electrical power), and are much more attractive. As a result, TPV, although interesting from a scientific point of view, has yet to gain traction as a viable option for the conversion of heat to electricity in a commercial context.

What is sometimes not realized at first glance, however, is that for emitter temperatures ~1300 °C, only 25% of the blackbody spectrum is usually above the TPV cell bandgap (~0.6–0.8 eV). Thus, if one considers only the portion of radiation above the band gap, rather than the full spectrum, the efficiencies become much more competitive. The problem is that unless a spectrally selective emitter is used, most refractory materials have substantial infrared (IR) emissivity and will therefore emit most of their radiation below the band gap. Thus, a critical challenge has been to develop a system level design concept that allows one to make maximum usage of the potential for high efficiency conversion of photons above the band gap, while disallowing the loss of the below band gap radiation, which manifests as absorption in the cell/module itself. This concept is generally referred to as photon recycling or spectral control, whereby photons with insufficient energy are reflected/recycled back to the emitter keeping it hot, and thus the energy is not lost. The notion of photon recycling has been around for many years,[13,23,39–54] but a full system that exploits the effect has, to our knowledge, yet to be analysed in detail to quantify exactly how much benefit it can provide. Such an analysis is the subject of the ensuing discussion.

In this respect, using a back surface reflector (BSR) to reflect unconvertable light back to the emitter is critical, and it is one of the primary distinctions between flat PV and TPV.[39,48–51] PV and TPV are in essence the same, in the sense that they utilize the photoelectric effect. However, in direct PV conversion of sunlight to electricity, one must attempt to convert a large portion of the spectrum to achieve high efficiency, because any reflected or absorbed photons below the band gap are lost, either by reflection to the surroundings or absorption in the cell and subsequent heat transfer to the environment. On the other hand, with TPV, one would prefer to reflect all photons below the band gap, since in a real system the emitter and cell have a high view factor and reflected photons will simply go back to the emitter. Thus, TPV only makes sense if one can implement effective spectral control, either on the side of the emitter, by only emitting photons above the band gap and/or by reflecting back photons below the band gap.

Considerable research has focused on engineering selective emitters[27,55–59] but it has been difficult to identify a material that can strongly suppress the below band gap radiation, as emissivities typically range from 0.05–0.4 beyond ~1 micron. Selective emitter coatings are further complicated by issues associated with thermal expansion matching of the coating and substrate, along with the cost of rare earth elements such as Er.[27,55–58] By contrast, materials such as silver (Ag) have much lower emissivity (*e.g.*, high reflectivity) in the far infrared *i.e.*, <1% absorption from $1 < \lambda < 30$ microns. Thus, it is likely to be much more efficient, reliable and cost effective to simply integrate a material such as Ag on the cold side (*e.g.*, the TPV cell) to reflect below band gap radiation back to the emitter, than to try and suppress long wavelengths from being emitted on the hot side.

The technique of using a BSR has been implemented previously and therefore in the ensuing analysis we have focused our discussion on the usage of TPV cells that are integrated with a high reflectivity (similar to Ag) BSR. The results of our analysis then quantify how important the BSR reflectivity is to the overall system performance, and to the best of our knowledge, no complete system level analysis incorporating spectral control and the specularity of the TPV cell BSR has been offered in the literature. Therefore, one objective of the present study is to present a more complete system level analysis of TPV with spectral control *via* BSR. The second objective is then to assess if a TPV system with TES could, under any circumstances, ever be competitive or provide advantages over turbines such as combined cycles, which can have efficiencies as high as ~60% and costs between \$1–2 $W^{-1}$. This becomes a critical question because unlike turbines, which currently operate very close to their thermodynamic efficiency limits,[60] other solid-state heat engine technologies, such as TPV, are much less developed and there is significant room for improvement.

## Using TPV as a power cycle for concentrated solar power (CSP) with thermal energy storage (TES)

One potential application for TPV has been in the context of solar energy conversion and specifically as a power cycle for CSP, instead of a turbine based heat engine. In CSP one first collects and concentrates sunlight, most often using reflectors, and then absorbs the light on what is termed a receiver. The receiver then transfers the thermal energy to another medium that can store heat inexpensively, typically a type of liquid (*i.e.*, molten salt) in tanks, which then acts as a thermal battery. The tanks are typically large, so that they lose a negligible fraction of the energy stored each day,[61–64] due to their large volume to surface area ratio. This is because the heat losses scale with the area exposed to the environment, while the energy stored scales with the volume. When electricity is needed the TES is discharged to feed the heat engine, often termed the power cycle, which converts the heat to electricity. Here it is important to appreciate that TES is one of the most attractive forms of energy storage, because it can be very inexpensive 4–10 times cheaper than electrochemical batteries, with extremely long lifetimes, near 100% thermal round trip efficiency, and the discharge rate is completely decoupled from the amount of energy stored. Furthermore, Denholm and co-workers[61,65–67] have performed detailed assessments of the value of adding TES, and have found that it can be particularly useful for higher penetration of renewables.

State of the art CSP plants with TES are capital intensive, but presently have a levelized cost of electricity (LCOE) in the range of ~13.5–20 cents per kWh.[68] Since LCOE scales with the inverse of the overall system efficiency (solar-to-electric), one potential route to decreasing the LCOE is to use a more efficient power cycle, since it is the largest source of inefficiency in the full system.[60] Current CSP power cycles are steam based Rankine cycles with an efficiency in the range of 35–40% and one potential way to improve the LCOE of CSP would be to consider using a solid-state heat engine such as TPV.[60] Here, the question is not only can one achieve a major boost in efficiency, but also whether it is possible to achieve a lower cost, faster response/ramp times/rates, longer life and lower maintenance costs than a turbine. It should be noted that the cost of the turbine in a CSP plant is not negligible as it is typically on the order of \$1 $W_e^{-1}$, while to total plant costs are typically ~\$4–6 $W_e^{-1}$.[68] However, by comparison, if the electrical power output of a TPV based power cycle was on the order of 50 $kW_e$ $m^{-2}$ of cell area and the cost of the cells could be reduced to the order of \$10 000 $m^{-2}$ *via* the use of reusable substrates, one could potentially achieve costs on the order of \$0.1 $W_e^{-1}$. Such an advancement would first require high efficiencies *e.g.*, >50% but would also require that such efficient cells be fabricated on reusable substrates. However, initial demonstrations by Morral *et al.*[69] suggest the possibility of such an advancement is not unfounded. Nonetheless, in the following, we outline how such a system might be designed and we analyse its performance to assess whether or not pursuing such an approach could ever be advantageous.

Considering the limits on TPV cell performance due to recombination,[70] one must operate the emitter at high temperatures so that (1) a material with a reasonably high band gap can be used, and (2) so that the heat flow from photons above the band gap greatly exceeds the rate of heat leakage to the environment. Generally, this corresponds to temperatures above 1000 °C, but one must also then think about what medium could be used to store the heat at such high temperatures. In this respect, we envision that one could use a TPV based power cycle in the context of CSP with TES, by using a receiver made of graphite, with liquid metal Sn serving as a primary heat transfer fluid (HTF).[71,72] Initial models and ongoing experiments suggest that this approach can reach the same range of receiver efficiencies as existing plants 80–90%, but would require higher sunlight concentrations >5000 kW $m^{-2}$. Furthermore, as has been confirmed by submerged sample experiments, Sn and graphite exhibit no chemical interaction at any temperature, despite the fact that they reside in the same column of the periodic table.[73] Thus, Sn(l) can be used as a HTF in a graphite piping network, since it melts at 232 °C and does not boil until 2602 °C, and will not exhibit any corrosion. Furthermore, commercial molten metal pumps made of graphite exist, and with proper retrofitting to keep the motor thermally isolated, they could be used at the requisite temperatures. Sn, however, is exceedingly expensive to use as a TES fluid, and therefore one must use another material to store the heat at high temperature.

Here, it should be appreciated that TPV, unlike a turbine, is best suited for a constant temperature heat input, similar to the idealized Carnot engine.[60] Therefore, the most exergetically efficient embodiment would be to store all of the heat at the highest possible temperature *via* a phase change material (PCM). It should be noted that a heat engine that takes in heat at a constant temperature has the potential to reach higher efficiencies than a heat engine that takes in heat over a range of temperatures, because there is less entropy transfer into the system.[60] Thus, a solid-state heat engine such as TPV has an intrinsic thermodynamic advantage over a turbine.[60]

There are very few classes of materials that are stable above 1000 °C, but there is one choice that can not only act as a PCM in the target temperature range, but also has a somewhat anomalously large heat of fusion and happens to be very low cost, namely silicon (Si). Si is the most abundant solid element on earth, with a cost for bulk metallurgical grade Si ~ \$1–2 per lb, a melting point of 1414 °C and a large heat of fusion of 1.92 MJ $kg^{-1}$. One could encapsulate Si in tubes made from inexpensive refractories, such as mullite or alumina stored in large, sealed closed end tubes, stacked in a larger tank. Here, the liquid metal Sn can flow in between the spaces between parallel tubes to either deliver or extract heat from the Si melting/solidification occurring inside the tubes. With such an approach, due to the extremely high convective heat transfer coefficients of liquid metals, the system could be operated near isothermally, with temperature differences on the order of 50 °C. It is also important to acknowledge that other embodiments could also work, but we have simply outlined one option here to illustrate that there is a pathway to realize such a system.

For example, as illustrated in Fig. 1, to charge the Si PCM TES, the Sn could be pumped to the receiver and heated from the melting point $T_{\mathrm{melt}}$ of the storage medium (Si − 1414 °C) to $\approx T_{\mathrm{melt}} + \Delta T_1$, *via* sensible heating. A high flow rate and small temperature rise $\Delta T \approx 50$ °C is needed to maximize the system level exergetic efficiency. The liquid Sn at $T_{\mathrm{melt}} + \Delta T_1$ could then be routed to the TES tank where it melts the storage medium and is cooled back to $T_{\mathrm{melt}}$, whereby it is recirculated back to the tower. To discharge the thermal battery, the Sn is then circulated from the TES tank to the power cycle. Here we envision a TPV based power cycle, which consists of a large

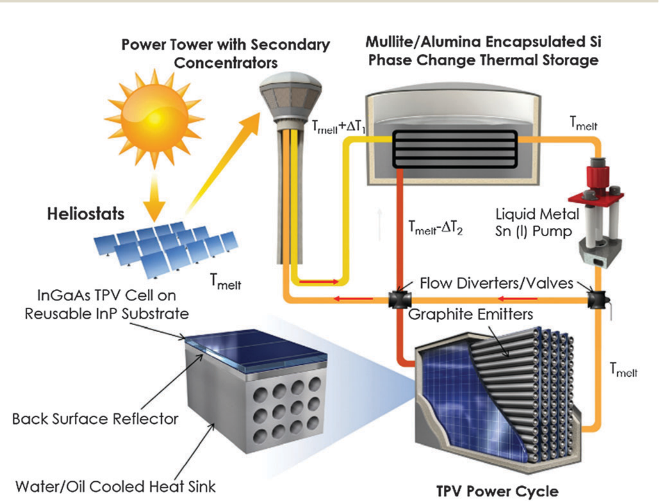


Fig. 1 Schematic conceptual layout of a utility scale TPV system. Red and white arrows on pipes indicate the flow path for charging (red) and discharging (white) the thermal storage.

array of graphite tubes that serve as near blackbody emitters. The TPV modules are located in between successive columns of graphite tubes and are irradiated with blackbody emission between $T_{\mathrm{melt}}$ and $T_{\mathrm{melt}} - \Delta T_2$, where again a small $\Delta T_2$ is used to preserve high exergetic efficiency and the heat is transferred to the emitter *via* sensible cooling in the Sn (see Fig. 1). A major benefit of using TES, aside from its low cost, is that dispatchability is enabled through the rate of discharge, which can be controlled by the flow rate of the Sn through the graphite emitter pipes (see Fig. 1).

In envisioning such a concept there is a critically enabling technology, namely the infrastructural components (*i.e.*, pumps, valves, flow meters *etc.*) that would be prerequisite. Although seemingly unrealistic at present, there is precedence to suggest that such a system could be successfully engineered if desired as well as initial demonstrations. Most notably a means of pumping the liquid metal, *via* a sump pump, already exists, albeit at lower temperatures.[74] Seal-less graphite sump pumps are available commercially and if retrofitted to thermally isolate the motor from the impeller, could operate at the temperature range of interest here. Such components are the subject of ongoing prototype development efforts, but essentially all of the key pieces exist, despite their need to be demonstrated together as a system. It is well acknowledged that such a concept would require continued development of these critical components, but in working towards their demonstration, it is nonetheless still useful to envision what other systems they can enable.

In the aforementioned system concept, the TPV modules would need to be engineered with the spectral control strategy integrated into the cell/module itself. High efficiency InGaAs cells[36] grown on reusable InP substrates[75] somehow backed with a highly reflective (*e.g.*, Ag) layer to serve as an inexpensive omnidirectional high efficiency IR reflector[76] is one potential option. This layer, along with the rest of the cell would then need to be engineered to minimize below band gap absorption and efficiently convert the upper 15–25% of the spectrum, which peaks between 1.72–1.97 microns (1200–1414 °C). The cells would then need to be actively cooled behind the substrates with a water or oil cooled heat sink keeping them at ambient temperature to maximize their performance. The entire power cycle unit would need to be heavily insulated from the environment and held in a vacuum to minimize convective and conductive heat leakage from the emitter (graphite pipes) to the TPV cells. Furthermore, the entire power cycle must be sufficiently large (*i.e.* $\approx$1–10 MW) to minimize edge effects and so the power generated inside greatly exceeds the heat leakage to the environment.

There are then several important questions to consider that will determine whether or not such a system could ever compete with turbine based heat engines: (1) how efficient could such a system be at scale and what are the most critical parameters? (2) How high of a back reflector reflectivity is required to reach competitive efficiencies? It is not clear *a priori* if realistic back reflector absorptivities (*e.g.*, 1–10%) are sufficiently low to enable competitive system level efficiencies, or if only extremely low reflectivities (<0.1%) can enable competitive efficiencies. (3) What length scale is necessary to minimize edge effects and suppress the heat losses to the environment? If system sizes much larger than 100 MW (typical power plant size) are required before the heat losses become a negligible fraction of the power generated, then this concept may never be viable due to excessively high capital costs. In the remaining sections we discuss a full 3D finite volume conjugate heat transfer model that treats the radiation *via* Monte Carlo ray tracing (MCRT). The model is used to answer these three primary questions and to obtain insights into what aspects might limit the system level performance.

## Computational model

In the model we seek the overall efficiency of a TPV power cycle, which is one subsystem of the envisioned CSP plant, where the efficiency is defined as the ratio of the electrical output *e.g.*, the product of open-circuit voltage, short-circuit current and fill factor ($\mathrm{FF}\cdot V_{\mathrm{OC}}\cdot I_{\mathrm{SC}}$) to the change in enthalpy (sensible heat) in the liquid Sn ($\dot{m}_{\mathrm{i}}C_{\mathrm{p}}(T_{\mathrm{out}} - T_{\mathrm{in}})$), which is the heat input. Here, it should be noted that henceforth the term "system efficiency" is used to refer to the power cycle subsystem efficiency in the CSP plant, which is useful for distinguishing it from the efficiency of sub-components such as the TPV cells or modules, which do not account for all of the losses in the power cycle subsystem. Steady state heat transfer calculations were performed by combining a spectral MCRT approach for calculation of the radiation between the emitter and TPV cells, with the conjugate Finite Volume Method (FVM) for solving the fluid flow and heat transfer in the liquid metal, graphite pipes and insulation. To reduce the temperature gradient and consequently the thermal stresses in the graphite tubes while also providing nearly constant temperature heat to the emitter, the liquid metal flow rate was chosen so that the temperature difference along the pipe's length is only ~50 °C. For such flow conditions the Reynolds number is >2300 hence we employed a turbulent model for Sn flow in the pipes. It should be noted, however, that the Sn convective heat transfer coefficient presents a negligible heat transfer resistance, even if the flow were laminar, due to its high thermal conductivity (>20 W m$^{-1}$ K$^{-1}$).[77] Consequently, the results are insensitive to the fluid flow model used. Thus, at every location in the Sn flow path, the temperature of the graphite containing the Sn is almost identical to the Sn temperature locally.

The heat equation is used to describe heat conduction through the insulation and pipe walls, and the MCRT approach is used to treat the radiation between the emitter and TPV cells/modules. The coupled radiation and fluid flow and heat transfer equations are solved iteratively and the high energy (above band gap – termed "in band") and lower energy (below the band gap – termed "out of band") radiative heat fluxes on the modules are obtained. Finally, using the External Quantum Efficiency (EQE) of the cell, the open-circuit voltage, current density and fill factor, as will be discussed, the output power and efficiency are calculated. Fig. 2 illustrates the power block

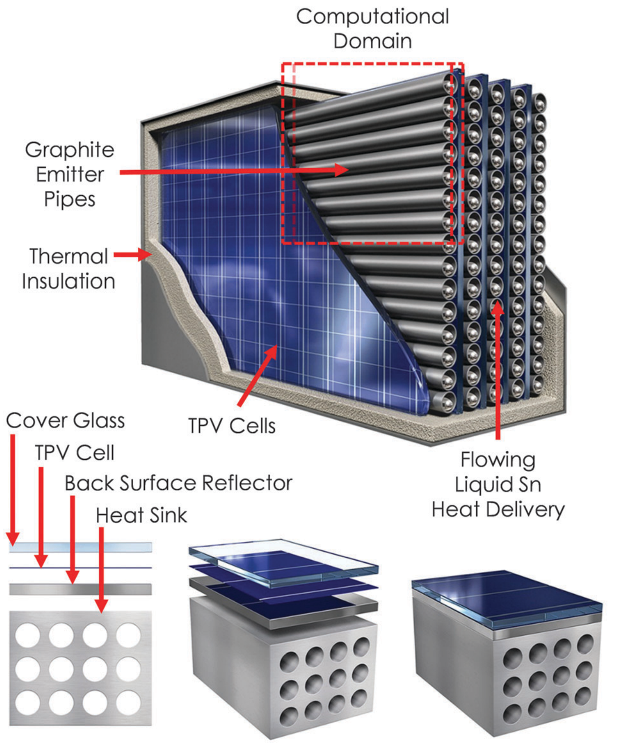


Fig. 2 Schematic illustrating (red dashed lines) the computational domain used in the model. The TPV module in front of graphite tubes is composed of many TPV cells connected in parallel and series. Contrary to the lines shown for illustrative purposes, the size of the cells should be small on the order of 0.1–1 $cm^2$ so that the resistive losses are minimized.

and computational domain used in this study. The overall efficiency of the system largely depends on the cell's EQE and the reflectivity of its integrated BSR. In an effort to assess what is achievable with current cells, as an example, we have used the EQE and voltage characteristics measured by Tuley *et al.*[36] for an InGaAs TPV cell grown on an InP substrate.

In order to calculate the output electrical energy from the system, the number of incident photons of a given energy is determined from the heat transfer simulation and then used along with the EQE of the TPV cell studied by Tuley *et al.*[36] The EQE represents the fraction of electrons collected per incident photon with a particular energy and therefore it measures how efficiently a cell can convert photons into electron hole pairs. The short-circuit current ($I_{SC}$) from the cell can be calculated by multiplying the EQE with the input radiation spectrum and integrating over the entire range of photon frequencies. The electrical power and the overall efficiency of the system can then be calculated using the fill factor (FF), which is the ratio of the maximum possible power obtained from the cell to the product of open-circuit voltage ($V_{OC}$) and short-circuit current.

$$P = N_{cell}V_{OC}I_{SC}FF \tag{2}$$

$$\eta = \frac{N_{cell}V_{OC}I_{SC}FF - \dot{W}_{cooling}}{Q_{in}} \tag{3}$$

Here, $N_{cell}$ is the number of TPV cells in the power block, $\dot{W}_{cooling}$ is the pumping power required by to actively cool the TPV cells/module, and $Q_{in}$ is the total energy input to the system which is the energy transferred from the Sn to the graphite tubes,

$$Q_{in} = \dot{m}C_p(T_{out} - T_{in}) \tag{4}$$

In eqn (4) $\dot{m}$ is mass flow rate of liquid metal Sn HTF in pipes, $C_p$ is specific heat, and $(T_{out} - T_{in})$ is the temperature difference between the inlet and outlet. Additional details of the computational model, validation of the model and further details associated with how the efficiency was calculated are included in the ESI.†

There are various losses that limit the performance of the TPV cells and modules themselves. Some of the loss mechanisms have overlap, but since the power output is proportional to the short-circuit current, open-circuit voltage and fill factor ($P \propto V_{OC}I_{SC}FF$), one can group them into three categories, namely (1) losses that decrease $I_{SC}$, (2) losses that reduce the $V_{OC}$, and (3) losses that decrease FF. The losses that decrease the short-circuit current are due to non-absorption of photons with energy lower than the bandgap energy, reflection of light from the top surface of the cell and contacts, transmission losses due to absorption of light in the bulk, area loss associated with metal electrode coverage and metal grid design, absorption of photons in the BSR, as well as photons that are absorbed onto the insulation and feed the heat leakage to the environment. The losses that reduce the open-circuit voltage are thermalization and collection losses due to bulk and surface recombination in the semiconductor as well as recombination in the depletion region. Lastly, the losses that reduce the fill factor are primarily resistive losses due to series and shunt resistance. It is worth mentioning that some of the aforementioned losses have multiple ramifications. For example, although the major effect of crystalline defects, impurities and incomplete chemical bonds is the reduction of open-circuit voltage, they can also have two other effects: (1) at high values of short-circuit current, impurities and defects act as traps for photoexcited carriers and recombination of these traps can result in the reduction of photocurrent and consequently short-circuit current, and (2) at low values of open-circuit voltages defects and impurities decrease the shunt resistance which results in a reduction in the fill factor. Another example is the overlap of collection and resistive losses. At high values of short-circuit current, the recombination in the depletion region increases both collection losses and resistive losses, which result in a reduction in open-circuit voltage and fill factor, respectively. Nonetheless, the aforementioned losses have been labelled according to the most significant effect they have on the efficiency.

Here, it is important to also note that the aforementioned losses can also be grouped into two distinct classifications, namely fundamental and practical losses. The only truly fundamental loss in TPV cells is radiative recombination which is unavoidable.[70] Other losses are practical losses which intrinsically have no lower bound and therefore in principle could be continually reduced through improved cell design and fabrication. For example, increasing the quality of semiconductor fabrication by reducing defects and impurities can minimize

Shockley–Read–Hall recombination and resistive losses due to shunt resistance. Also, cell/module series resistance can be minimized using new and innovative approaches, such as multilevel interconnection designs,[78,79] tandem/multi-junction devices,[80,81] vertical multi-junction (VMJ) cell structures,[82,83] and Monolithically Integrated Modules (MIM).[84–92] It is worth mentioning that the reported series resistance values of some the best fabricated cells for concentrated and non-concentrated PV are between 0.1–2 m$\Omega$ cm$^2$.[93–102] Given this distinction between fundamental and practical losses, in the subsequent analysis we consider three primary example cases for the TPV cells/modules: (case 1) where $V_{OC}$, $I_{SC}$ and FF are determined from the experimental current voltage curve and wavelength dependent EQE of an InGaAs–InP cell studied by Tuley *et al.*,[36] (case 2) where we consider the upper limits for $V_{OC}$, $I_{SC}$, and FF, by neglecting all the losses that are associated with the cell design and fabrication, and (case 3) where we incorporate series resistance into case 2, since it is one of the most important practical losses in the cells.

For all cases, the emitter temperature was determined by the heat transfer calculation, where the inlet temperature for the Sn(l) was held constant at 1750 K. This yielded almost a constant temperature emitter, which provided a photon flux above the band gap of 109 kW m$^{-2}$ (10.9 W cm$^{-2}$) and 315 kW m$^{-2}$ (31.5 W cm$^{-2}$) below the band gap. Thus, the net photon flux was 42.4 W cm$^{-2}$, which is the same as a concentration factor of $\sim$420$\times$ for a cell directly illuminated with concentrated sunlight. For case 1, all the losses due to recombination, series resistance, transmission, reflection, area loss, and so on are considered in the calculation by using the experimental data of series resistance and wavelength dependent EQE, as well as ideal and non-ideal dark saturation currents.[36] The values of all intrinsic cell parameters in the equation such as ideal and space charge non-ideal dark saturation currents are obtained by fitting a double diode model to the experimental *I–V* curve as discussed in the ESI.† The photocurrent is calculated using experimental data for EQE first. Then the $V_{OC}$ is obtained by numerical solution of the two diode equation. Finally, the maximum power point and consequently the fill factor are calculated by numerical solution of the derivative of the *I–V* curve, *i.e.*, $\frac{dI}{dV} = 0$. For cases 2 and 3, it is assumed that the EQE = 1 for all photons above the band gap energy and we assume the TPV cell operates at its maximum open-circuit voltage, *i.e.*, $V_{OC} = V_{max}$ at room temperature (300 K). For cases 2 and 3 the maximum open-circuit voltage at 300 K, fill factor and the effect of the series and shunt resistances on the fill factor are calculated using the relations developed by Green[103,104] and Kiess and Rehwald.[105] For more details on the calculation procedure, readers are referred to the ESI,† but the purpose of examining all three cases is to assess where the current state of the art is (case 1), and how much room exists for improvement (cases 2 and 3). Also, in the forthcoming results, the BSR reflectivity was treated as a variable so that we could examine how strongly the power cycle system efficiency affected by its value. The range for BSR reflectivity values ranged from zero, which yields the full-spectrum efficiency, to unity, which yields the monochromatic efficiency.

It is also important to emphasize that since the TPV cell operates at high concentration levels, the cell temperature can significantly increase beyond the room temperature if it is not actively cooled. However, it is very straightforward to keep the cell temperature within 2 °C of the ambient temperature using active cooling from a liquid such as water or a heat transfer oil as well as a heat sink to increase the surface area of contact between the cell and liquid. As shown in the ESI,† a simple, easy to fabricate, and low cost copper-water cooling system can remove the heat from the system and maintain the temperature of the cell/module below 302 K with negligible pumping power required to circulate the coolant through the system.

## Results and discussion

One source of potential inefficiency at the system level that was not discussed in the preceding section is associated with non-uniform radiation, which causes some of the TPV modules to output less electricity (*e.g.*, edge effects). Although one can intuitively reason that large aspect ratios should be less affected by such edge effects, it was not clear *a priori*, how large an aspect ratio is required. We therefore calculated the heat fluxes on the surface of TPV modules, normalized by their maximum values as discussed in the ESI.† The two important aspect ratios are denoted as $AR_H = H/C$ and $AR_L = L/C$. They represent the ratio between the overall height of the system ($H$) and the length of the system ($L$) to the distance between the modules and tubes ($C$). These aspect ratios were varied to determine how large $AR_L$ and $AR_H$ must be to approach the infinite system size limit. As discussed in the ESI,† aspect ratios beyond 40 yield negligible differences with respect to the infinite system size limit (*i.e.*, uniform flux). Thus, in the ensuing analysis, the same heat flux distribution and average values for heat fluxes obtained for the system with an aspect ratio of 50 are used for all remaining calculations.

In order to address the issue of heat leakage to the environment through the insulation, we examined how the efficiency scaled with the overall system size when including heat leakage through the insulation. The heat loss due to conduction through the insulation and subsequent convection and radiation to the surroundings can be easily estimated using a simple thermal resistance circuit as follows,

$$Q_{\mathrm{loss},1} = \frac{T_{\mathrm{inner}} - T_{\infty}}{R_{\mathrm{total}}} \tag{5}$$

where $T_{\infty}$ and $T_{\mathrm{inner}}$ are the surrounding environment's ambient temperature and the average temperature of the inner surface of the insulation respectively. In eqn (5) $R_{\mathrm{total}}$ is the total thermal resistance between the inner surface of the insulation and the surroundings which can be expressed as

$$R_{\mathrm{total}} = \frac{t}{k_{\mathrm{ins}} A_{\mathrm{i}}} + \left(\frac{1}{h_{\infty} A_{\mathrm{o}}} + \frac{1}{h_{\mathrm{r}} A_{\mathrm{o}}}\right)^{-1} \tag{6}$$

where $A_i$, $A_o$, $t$ and $k_{ins}$ are internal and external surface area of the insulation, its thickness and thermal conductivity respectively. In eqn (6), the effective combined convective and radiative heat transfer coefficient outside of the power block is given by $h_r = \sigma\,\varepsilon_{ins}\,(T_{outer} + T_{inner})(T_{outer}{}^2 + T_{inner}{}^2)$, where $\varepsilon_{ins}$ and $T_{outer}$ are the emissivity and the outer surface temperature of the insulation, respectively. The energy balance in the TPV block then results in the following expression for the system efficiency,

$$\eta = 1 - \frac{Q_{loss,tot}}{\dot{m}C_p(T_{out} - T_{in})} \quad (7)$$

where $Q_{loss,tot} = Q_{loss,1} + Q_{waste}$ is the total heat loss to the environment. Here, $Q_{loss}$ is the total heat loss through the insulation and $Q_{waste}$ is the waste heat absorbed/rejected in the TPV modules, which is ultimately transferred to the environment *via* the active cooling system. The quantity $Q_{waste}$ is the product of the below band gap radiative heat flux and TPV cell absorptivity along with the other cell/module level losses.

Although the photoelectric effect itself is essentially size independent, the overall performance of a TPV power cycle system is strongly size dependent. This is because one must insulate the emitter from the environment, which is most effectively accomplished with porous solid insulation. Nonetheless, eqn (6) and (7) show that the efficiency of the system is proportional to the volume to surface area ratio, because the electrical output scales with the system volume, while the heat leakage scales with the system's surface area. Thus, despite many efforts to exploit the size independence of the photoelectric effect in TPV, one cannot circumvent the need to insulate the emitter from the environment, which enjoins a dependence on the volume to surface area ratio. Fig. 3 shows that the efficiency increases with increasing volume to surface area ratio ($\phi = V/A$) due to the fact that at higher $\phi$, the heat leakage from the system is small compared to the power generated internally. In order to minimize these losses and maximize the efficiency, system sizes on the order of 1 m are required. This is a very important result, as many applications of TPV often focus on its ability to operate at small scales efficiently as a principle benefit.[106] Our results, here, however, suggest that at small scales, on the order of 0.1 m or less, the system level efficiency will still exhibit strong size effects, despite the fact that the underlying photoelectric effect itself is essentially size independent. This limitation ultimately arises due to the lower bounding limitations on the thermal conductivity of insulation, which is on the order of 0.01 W m$^{-1}$ K$^{-1}$. This then necessitates a certain thickness of insulation to prevent heat loss and small systems do not generate enough power to greatly outweigh this essentially fixed heat flux. Fig. 3 therefore shows that operating a TPV power cycle at a sufficiently large scale is the most important step that must be made towards improving the efficiency. It is also critically important to realize that by simply increasing the size one relinquishes a common goal in TPV cell design, which is to use lower band gap materials so that more of the emitter radiation is above the band gap. This has the effect of increasing the power output per unit active area, but the primary reason this is necessary, other than cost considerations, is to compete with the heat leakage to the environment. However, if one settles this competition by simply making the system large enough, the choice of TPV cell material can shift to materials with higher band gaps and lower power output per unit active area, to achieve higher efficiency.

Fig. 4 shows that integrating a spectral control strategy for recycling the low energy photons is the next most important barrier to improving the efficiency of the cells/modules. In Fig. 4, we have quantified the system efficiency as a function of the BSR reflectivity for the three base cases. For the real InGaAs cell with FSE = 12.4% at $T_E$ = 3250 K, it can be seen that increasing the BSR reflectivity from 0 (no BSR) to 1 results in $>2\times$ increase in efficiency. Thus, it is clear that integrating a high reflectivity BSR can have a dramatic effect on increasing the overall power cycle efficiency.

Here, it is worth noting that the Internal Fluorescence Efficiency ($\eta_{IFE}$) which is the ratio between the radiative recombination rate ($U_{radiative}$) and the total recombination rate in the cell ($U_{non\text{-}radiative} + U_{radiative}$), *i.e.*, $\eta_{IFE} = \frac{U_{radiative}}{U_{non\text{-}radiative} + U_{radiative}}$, quantifies the degree of non-radiative recombination losses in

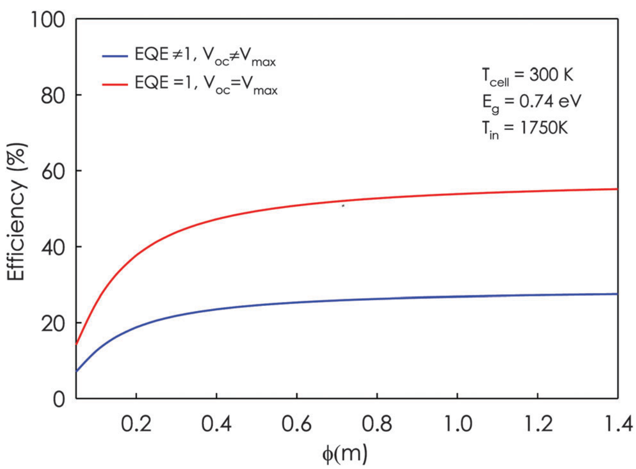


Fig. 3 Effect of volume to surface area of TVP block efficiency.

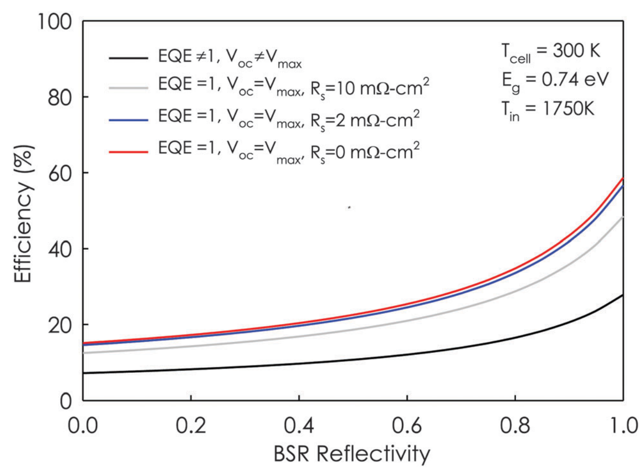


Fig. 4 Effect of BSR reflectivity on TPV efficiency.

 

the TPV cell.[107,108] Throughout this study, in calculating the upper limiting efficiency for the power block it has been assumed that radiative recombination is the dominant recombination channel in the TPV cell. However, practically, parasitic photon absorption in non-photoactive layers of the cell and non-radiative recombination can strongly affect the TPV cell's performance depending on the doping level, fabrication process, cell bandgap, and injection level or excess carrier concentration. The reduction of the open circuit voltage due to non-radiative recombination and parasitic photon absorption losses can be related to the External Luminescent Efficiency ($\eta_{\mathrm{EFE}}$),[108,109] which quantifies the fraction of internally emitted photons that are ultimately able to escape through the front surface of the TPV cell.[107–109] The cell architecture and consequently $\eta_{\mathrm{EFE}}$ play an important role on the overall efficiency of power block, which should be taken into account when estimating the effects of non-radiative recombination in an actual cell. It has been shown, however, that improved cell level optical management can decrease the gap between $\eta_{\mathrm{IFE}}$ and $\eta_{\mathrm{EFE}}$.[108,109] For example, a very high BSR reflectivity can significantly increase the cell $\eta_{\mathrm{EFE}}$, thereby decreasing the gap between $\eta_{\mathrm{IFE}}$ and $\eta_{\mathrm{EFE}}$.[108,109] Therefore, high BSR reflectivity is extremely important, because it not only has the impact illustrated in Fig. 4, but it can also significantly affect the cell performance.

Lastly, it is important to realize that if these first two strategies are implemented, namely that large system sizes are constructed and a high reflectivity BSR is integrated, the priorities for further optimization change. For example, when considering the real cell data used,[36] the EQE between 0.4–0.87 microns drops well below 60%. For a cell with no BSR these photons represent such a small fraction of the power output, they might be viewed with little priority. However, when one integrates a BSR, the priorities for further optimization change, and the path to further increasing efficiency involves maximizing the collection (EQE) and voltage associated with the photons with energies significantly above the band gap. This might then suggest that further optical filtering, or multiple junctions could provide some additional benefits. For example, consider the results for the idealized case 2, in Fig. 3 and 4 which reach 59% at a large scale and high BSR reflectivity. With an efficiency of 59%, it becomes interesting to consider what is responsible for the remaining ($\sim$41%) of the energy loss during conversion. There are three losses that contribute to the remaining $\sim$41%, namely the voltage drop and fill factor loss (23%), and the thermalization loss (18%). The first loss is strongly a function of the operating temperature of the cell and is unlikely to be overcome, unless the cell is somehow actively cooled below the ambient temperature, which would require a parasitic power draw that would reduce the net efficiency. The fill factor loss is affected by cell's resistance, which could potentially be improved through optimization, but would depend on the details of a given cell. Thermalization losses, however, account for almost half of the remaining 41%, and in concept, this loss can be further reduced by situating the cell optically in series or adding more junctions to extract the energy of higher energy photons first, as is commonly done in multi-junction PV cells.[81,110–112]

To roughly estimate how much additional benefit could be obtained by using different materials with different band gaps in series, the simplest approach would be to situate the cells optically in series, but treat them as electrically independent. This is because multi-junction cell optimization includes many additional considerations.[113] Nonetheless, to provide an approximate picture of how much could be gained by adding a top cell with a higher band gap and the InGaAs cell in tandem, we have computed the overall efficiency of a system with two cells for cases 2 and 3. Fig. 5 shows that there is an optimum bandgap ($E_{g2} \sim 0.94$ eV) for the top material that yields the maximum efficiency. This optimum occurs because of the relative trade-off between thermalization losses in the bottom cell (InGaAs cell) *vs.* the fictitious topping cell. The addition of this second TPV cell increases the overall efficiency by an additional 5% indicating that the potential exists to cross the critical barrier of 60%[114,115] and conceptually, additional materials could increase this even more.

The significance of the 60% barrier is important, because it represents the highest heat engine efficiency that has ever been achieved commercially, which is accomplished through the usage of a tandem/combined (Brayton + Rankine) turbine based cycle. Turbomachinery based heat engines are the most efficient and cost effective heat engines at present and are therefore the most widely used devices in the utility-scale power generation industry. Their costs are well-established and unlikely to see significant decreases in the future, and their performance is limited by thermodynamics – which is fundamental. Henry and Prasher,[60] for example, have shown that turbines currently operate very close to their fundamental thermodynamic limits and thus there is little room for significant improvement, other than increasing the operating temperatures. From this perspective, it is then quite remarkable to note that TPV may have the potential to one day reach the same or possibly higher performance than a combined cycle. Unlike, turbine engineering, which has been highly successful over the last few decades and has already capitalized on most opportunities for further

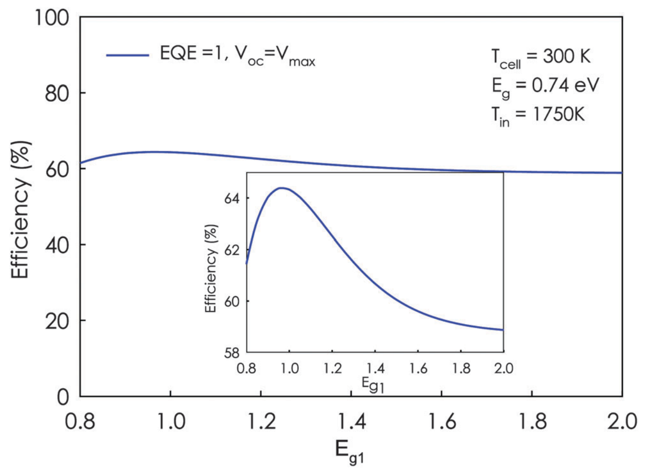


Fig. 5 System efficiency for a dual junction TPV cell. The inset shows the peak in efficiency at 0.95 eV.

advancement, TPV has much more room for improvement. Thus, it is remarkable to consider TPV as an alternative power cycle for CSP or grid scale storage applications, particularly given its potential to cost 2–10× less than a turbine. Furthermore, it is interesting to consider the additional advantages associated with using a TPV power cycle at the utility scale. For example, one could imagine arranging the TPV cells in such a way that that they can be mechanically moved into and out of view of the emitter. In this way, one could control the output of the system and shift from zero to full load within seconds, which could allow for load following of other renewables, providing the grid with great flexibility.

## Conclusions

In this paper, we modelled a TPV system that receives heat from a TES system and thus, has the potential to provide dispatchable electricity. The usage of a liquid metal heat transfer fluid such as Sn and a TES system based on Si is critical to enabling the heat delivery. The system level analysis then enabled identification of the most important design parameters that affect the overall power cycle system efficiency. The results suggest that amongst the major steps towards improving the efficiency of a TPV system, building systems at sufficiently large scales and integrating a high reflectivity BSR are the most important and significant improvements one can make. The next most important improvement, assuming the first two improvements are implemented, is increasing the EQE for photons above the band gap and possibly using multi-junction or multiple TPV cells arranged optically in series to reduce thermalization losses. If these strategies are implemented, the model remarkably shows that TPV may have the potential to reach/exceed the efficiencies of combined cycles (∼60%). Lastly, one of the most important benefits that could be derived from using TPV as opposed to a mechanical heat engine, is cost. Turbine costs are well-established and are in the range of $1–2 $W^{-1}$, with no pathway for order of magnitude improvements. However, TPV cells, if fabricated on reusable substrates and produced at high volume have a pathway to reach costs an order of magnitude lower (∼$0.1 $W^{-1}$). Such a major cost reduction could make renewable technologies such as CSP more competitive with fossil fuel alternatives and therefore deserve further study and examination.

The system that was modelled shows great potential, but will require further technological advancements to be realized. Most notably, initial laboratory scale demonstrations of all ceramic circulation loops have been recently demonstrated (publications in progress), including pumps, valves and materials testing to verify the absence of material degradation/chemical interaction at such high temperatures. Nonetheless, further testing and larger scale demonstrations are needed. Demonstrating that light can be efficiently concentrated and converted to heat in a receiver at such high temperatures is still needed/ongoing, but initial models suggest high efficiencies (80–90%) are attainable.[116] Nonetheless, there is strong evidence to suggest that the thermal side of the system analysed herein can be realized and will be cost effective, which is what initially prompted this investigation.

More development is also needed on the side of the TPV cells/modules. First, it is important to demonstrate that such a high efficiency is possible, by re-engineering cells/modules to include a high reflectivity BSR, and the cells must be optimized to leverage this by placing the strongest emphasis on above band gap EQE, rather than lowering the band gap to convert a greater portion of the spectrum. It may also be advantageous to investigate the benefits of multi-junction TPV cells and it will be important to consider series resistance issues in the design of optimized cells. This, however, would require a dedicated effort that is focused on the cell/module level priorities, which should be dictated by the larger system level performance model. Lastly, an absolutely imperative step towards making the outlined approach viable, is reducing the cell/module cost to the order of $10 000 $m^{-2}$. Reaching this cost target has yet to be demonstrated, but seems feasible if an approach that involves reusable substrates is employed, which has been demonstrated.[69,75] Overcoming all of these challenges would require a major research and development (R&D) effort sustained over many years, but it is important to keep in perspective that such efforts have been pursued for other heat engine technologies, namely turbines. However, the key distinction between turbines and the system analysed herein is the potential room for improvement. Turbomachinery based heat engines have minimal prospects for further improvement, while TPV has several potential avenues for improvement, and therefore to justify such a large R&D effort, it is useful to outline what is possible, as has been undertaken in the present study.

## Acknowledgements

This project was supported by DOE ARPA-E, grant number DE-AR0000339.

## References

1 B. D. Wedlock, *Proc. IEEE*, 1963, **51**, 694–698.
2 J. Yeargan, R. Cook and F. Sexton, *12th Photovoltaic Specialists Conference*, 1976, 807–813.
3 F. Demichelis and E. Minettimezzetti, *Sol. Cells*, 1980, **1**, 395–403.
4 P. Wurfel and W. Ruppel, *IEEE Trans. Electron Devices*, 1980, **27**, 745–750.
5 R. M. Swanson, in *Photovoltaic Solar Energy Conference*, ed. W. Palz, Springer, Netherlands, 1981, ch. 185, pp. 1097–1097.
6 P. A. Davies and A. Luque, *Sol. Energy Mater. Sol. Cells*, 1994, **33**, 11–22.
7 L. M. Fraas, H. H. Xiang, S. Hui, L. Ferguson, J. Samaras, R. Ballantyne, M. Seal and E. West, *AIP Conf. Proc.*, 1996, **358**, 128–133.
8 L. J. Ostrowski, U. C. Pernisz and L. M. Fraas, *AIP Conf. Proc.*, 1996, **358**, 251–260.

 

9 A. Schock, C. Or and V. Kumar, *AIP Conf. Proc.*, 1996, **358**, 81–97.
10 K. W. Stone, D. L. Chubb, D. M. Wilt and M. W. Wanlass, *AIP Conf. Proc.*, 1996, **358**, 199–209.
11 C. L. DeBellis, M. V. Scotto, S. W. Scoles and L. Fraas, *Thermophotovoltaic Generation of Electricity*, 1997, **401**, 355–367.
12 M. Wanlass, J. Carapella, A. Duda, K. Emery, L. Gedvilas, T. Moriarty, J. Ward, J. Webb, X. Wu and C. Murray, presented in part at the Fourth NREL Conference, 1998.
13 T. J. Coutts, *Renewable Sustainable Energy Rev.*, 1999, **3**, 77–184.
14 O. Morrison, M. Seal, E. West and W. Connelly, *Thermophotovoltaic Generation of Electricity*, 1999, **460**, 488–496.
15 T. J. Coutts, *Sol. Energy Mater. Sol. Cells*, 2001, **66**, 443–452.
16 O. V. Sulima and A. W. Bett, *Sol. Energy Mater. Sol. Cells*, 2001, **66**, 533–540.
17 L. M. Fraas, J. E. Avery and H. Han Xiang, presented in part at the Photovoltaic Specialists Conference, 19–24 May 2002.
18 O. M. Nielsen, L. R. Arana, C. D. Baertsch, K. F. Jensen and M. A. Schmidt, presented in part at the The 12th international Conference on Solid Stale Sensors, Actuators and Microsystems, June 8–12, 2003.
19 W. M. Yang, S. K. Chou, C. Shu, Z. W. Li and H. Xue, *Sol. Energy Mater. Sol. Cells*, 2003, **80**, 95–104.
20 T. Bauer, I. Forbes and N. Pearsall, *Int. J. Ambient Energy*, 2004, **25**, 19–25.
21 S. Bitnar, W. Durisch, G. Palfinger, F. von Roth, U. Vogt, A. Bronstrup and D. Seiler, *Semiconductors*, 2004, **38**, 941–945.
22 B. P. Davenport and S. Michael, *Advanced thermophotovoltaic cells modeling, optimized for use in radioisotope thermoelectric generators (RTGs) for Mars and deep space missions*, Defense Technical Information Center, 2004.
23 B. Wernsman, R. R. Siergiej, S. D. Link, R. G. Mahorter, M. N. Palmisiano, R. J. Wehrer, R. W. Schultz, G. P. Schmuck, R. L. Messham, S. Murray, C. S. Murray, F. Newman, D. Taylor, D. M. DePoy and T. Rahmlow, *IEEE Trans. Electron Devices*, 2004, **51**, 512–515.
24 C. J. Crowley, N. A. Elkouh, S. Murray and D. L. Chubb, *Space Technology and Applications International Forum-Staif 2005*, 2005, **746**, 601–614.
25 B. Wernsman, R. G. Mahorter, R. Siergiej, S. D. Link, R. J. Wehrer, S. J. Belanger, P. Fourspring, S. Murray, F. Newman, D. Taylor and T. Rahmlow, *Space Technology and Applications International Forum*-Staif 2005, 2005, **746**, 1441–1448.
26 D. Chubb, *Fundamentals of thermophotovoltaic energy conversion*, Elsevier, 2007.
27 G. Mattarolo, *Development and modelling of a thermophotovoltaic system*, Kassel university press, 2007.
28 V. L. Teofilo, P. Choong, J. Chang, Y. L. Tseng and S. Ermer, *J. Phys. Chem. C*, 2008, **112**, 7841–7845.
29 P. Bermel, M. Ghebrebrhan, W. Chan, Y. X. Yeng, M. Araghchini, R. Hamam, C. H. Marton, K. F. Jensen, M. Soljacic, J. D. Joannopoulos, S. G. Johnson and I. Celanovic, *Opt. Express*, 2010, **18**(suppl 3), A314–A334.
30 T. Bauer, *Thermophotovoltaics: basic principles and critical aspects of system design*, Springer Science & Business Media, 2011.
31 M. Bosi, C. Ferrari, F. Melino, M. Pinelli, P. Spina and M. Venturini, *Proceedings ECOS*, 2012.
32 W. R. Chan, P. Bermel, R. C. Pilawa-Podgurski, C. H. Marton, K. F. Jensen, J. J. Senkevich, J. D. Joannopoulos, M. Soljacic and I. Celanovic, *Proc. Natl. Acad. Sci. U. S. A.*, 2013, **110**, 5309–5314.
33 C. Ferrari, F. Melino, M. Pinelli and P. R. Spina, *Appl. Energy*, 2014, **113**, 1717–1730.
34 C. Ferrari, F. Melino, M. Pinelli, P. R. Spina and M. Venturini, *Energy Procedia*, 2014, **45**, 160–169.
35 A. Lenert, Y. Nam, D. M. Bierman and E. N. Wang, *Opt. Express*, 2014, **22**(suppl 6), A1604–A1618.
36 R. S. Tuley, J. M. S. Orr, R. J. Nicholas, D. C. Rogers, P. J. Cannard and S. Dosanjh, *Semicond. Sci. Technol.*, 2013, **28**, 015013.
37 D. M. Wilt, N. S. Fatemi, R. W. Hoffman, P. P. Jenkins, D. J. Brinker, D. Scheiman, R. Lowe, M. Fauer and R. K. Jain, *Appl. Phys. Lett.*, 1994, **64**, 2415–2417.
38 S. Wojtczuk, E. Gagnon, L. Geoffroy and T. Parodos, *AIP Conf. Proc.*, 1995, **321**, 177–187.
39 R. R. Siergiej, B. Wernsman, S. A. Derry, R. G. Mahorter, R. J. Wehrer, S. D. Link, M. N. Palmisiano, R. L. Messham, S. B. Murray, C. S. Murray, F. Newman, J. Hills and D. Taylor, *Thermophotovoltaic Generation of Electricity*, 2003, **653**, 414–423.
40 G. W. Charache, D. M. DePoy, P. F. Baldasaro and B. C. Campbell, *AIP Conf. Proc.*, 1996, **358**, 339–350.
41 P. Iles and C. Chu, presented in part at the The 2nd NREL conference on thermophotovoltaic generation of electricity, 1996.
42 D. M. Wilt, N. S. Fatemi, P. P. Jenkins, R. W. Hoffman, Jr., G. A. Landis and R. K. Jain, presented in part at the Photovoltaic Specialists Conference, 13–17 May 1996, 1996.
43 M. G. Mauk, Z. A. Shellenbarger, M. I. Gottfried, J. A. Cox, B. W. Feyock, J. B. McNeely, L. C. DiNetta and R. L. Mueller, *Thermophotovoltaic Generation of Electricity*, 1997, **401**, 129–137.
44 M. B. Clevenger, C. S. Murray, S. A. Ringel, R. N. Sacks, L. Qin, G. W. Charache and D. M. Depoy, *Thermophotovoltaic Generation of Electricity*, 1999, **460**, 327–334.
45 J. M. Borrego, S. Saroop, R. J. Gutmann, G. W. Charache, T. Donovan, P. F. Baldasaro and C. A. Wang, *J. Appl. Phys.*, 2001, **89**, 3753–3759.
46 M. G. Mauk and V. M. Andreev, *Semicond. Sci. Technol.*, 2003, **18**, S191–S201.
47 D. DePoy, P. Fourspring, P. Baldasaro, J. Beausang, E. Brown, M. Dashiel, K. Rahner, T. Rahmlow, J. Lazo-Wasem and E. Gratrix, *LM-04K053, June*, 2004, **9**.
48 R. K. Huang, C. A. Wang, M. K. Connors, G. W. Turner and M. Dashiell, *Thermophotovoltaic Generation of Electricity*, 2004, **738**, 329–336.
49 P. M. Fourspring, D. M. DePoy, J. F. Beausang, E. J. Gratrix, R. T. Kristensen, T. D. Rahmlow, P. J. Talamo,

J. E. Lazo-Wasem and B. Wernsman, *Thermophotovoltaic Generation of Electricity*, 2004, **738**, 171–179.
50 L. B. Karlina, M. M. Kulagina, N. K. Timoshina, A. S. Vlasov and V. M. Andreev, *AIP Conf. Proc.*, 2007, **890**, 182–189.
51 Z. A. Shellenbarger, G. C. Taylor, R. U. Martinelli and J. A. Carpinelli, *Thermophotovoltaic Generation of Electricity*, 2004, **738**, 345–352.
52 R. E. Black, P. F. Baldasaro and G. W. Charache, presented in part at the Eighteenth International Conference on Thermoelectrics., Baltimore, MD, USA, Aug. 29-Sept. 2 1999.
53 U. Ortabasi, *AIP Conf. Proc.*, 2003, **653**, 249–258.
54 T. D. Rahmlow, D. M. DePoy, P. M. Fourspring, H. Ehsani, J. E. Lazo-Waseml and E. J. Gratrix, *Thermophotovoltaic Generation of Electricity*, 2007, **890**, 59–67.
55 G. E. Guazzoni, *Appl. Spectrosc.*, 1972, **26**, 60–65.
56 H. J. Wang, H. Ye and Y. Z. Zhang, *Sci. China: Technol. Sci.*, 2014, **57**, 332–338.
57 D. L. Chubb, A. T. Pal, M. O. Patton and P. P. Jenkins, *J. Eur. Ceram. Soc.*, 1999, **19**, 2551–2562.
58 J. M. Gee, J. B. Moreno, S. Lin and J. G. Fleming, presented in part at the Photovoltaic Specialists Conference, Conference Record of the Twenty-Ninth IEEE, 19–24 May 2002.
59 B. Bitnar, W. Durisch, J. C. Mayor, H. Sigg and H. R. Tschudi, *Sol. Energy Mater. Sol. Cells*, 2002, **73**, 221–234.
60 A. Henry and R. Prasher, *Energy Environ. Sci.*, 2014, **7**, 1819–1828.
61 S. H. Madaeni, R. Sioshansi and P. Denholm, *Proc. IEEE*, 2012, **100**, 335–347.
62 S. H. Madaeni, R. Sioshansi and P. Denholm, *Contract*, 2011, **303**, 275–3000.
63 J. Jorgenson, P. Denholm and M. Mehos, presented in part at the Proceedings of the ASME 2014 8th International Conference on Energy Sustainability June 30-July 2, 2014.
64 M. Hummon, P. Denholm, J. Jorgenson and M. Mehos, *3rd Workshop of Integration of Solar Power into Power Systems*, 2013, pp. 20–21.
65 S. H. Madaeni, R. Sioshansi and P. Denholm, *IEEE Trans. Power Syst.*, 2012, **27**, 1116–1124.
66 P. Denholm and M. Hand, *Energy Policy*, 2011, **39**, 1817–1830.
67 R. Sioshansi and P. Denholm, *IEEE Trans. Sustain Energy*, 2010, **1**, 173–183.
68 US Department of Energy, SunShot Vision Study, 2012.
69 A. Fontcuberta Morral, J. Zahler, H. A. Atwater, S. Ahrenkiel and M. Wanlass, *Appl. Phys. Lett.*, 2003, **83**, 5413.
70 W. Shockley and H. J. Queisser, *J. Appl. Phys.*, 1961, **32**, 510–519.
71 C. S. Yuan, C. Jarrett, W. Chueh, Y. Kawajiri and A. Henry, *Sol. Energy*, 2015, **122**, 547–561.
72 C. Yuan, C. Jarrett, W. Chueh, Y. Kawajiri and A. Henry, *J. Therm. Eng.*, 2015, **2**, 837–852.
73 E. L. Reed, *J. Am. Ceram. Soc.*, 1954, **37**, 146–153.
74 http://www.mmei-inc.com/.
75 J. M. Zahler, K. Tanabe, C. Ladous, T. Pinnington, F. D. Newman and H. A. Atwater, *Appl. Phys. Lett.*, 2007, **91**, 012108.
76 B. Wernsman, R. R. Siergiej, S. D. Link, R. G. Mahorter, M. N. Palmisiano, R. J. Wehrer, R. W. Schultz, G. P. Schmuck, R. L. Messham, S. Murray, C. S. Murray, F. Newman, D. Taylor, D. M. DePoy and T. Rahmlow, *IEEE Trans. Electron Devices*, 2004, **51**, 512–515.
77 S. Sharafat and N. Ghoniem, *Summary of Thermo-Physical Properties of Sn, And Compounds of Sn-H, Sn-O, Sn-C, Sn-Li, and Sn-Si And Comparison of Properties of Sn, Sn-Li, Li, and Pb-Li*, M. A. E. Dept, University of California, Los Angles, 2000.
78 P. Verlinden, R. A. Sinton and R. M. Swanson, *Int. J. Sol. Energy*, 1988, **6**, 347–366.
79 P. Verlinden, R. M. Swanson, R. A. Sinton and D. E. Kane, Photovoltaic Specialists Conference, Las Vegas, NV, USA, Sep. 26–Sep. 30, 1988.
80 B. E. Sağol, N. Szabo, H. Döscher, C. Höhn, K. Schwarzburg and T. Hannappel, http://www.quantsol.org/pub/pub09_26.pdf.
81 H. Cotal, C. Fetzer, J. Boisvert, G. Kinsey, R. King, P. Hebert, H. Yoon and N. Karam, *Energy Environ. Sci.*, 2009, **2**, 174–192.
82 J. Goodrich, J. Chapple-Sokol, G. Allendorf and R. Frank, *Sol. Cells*, 1982, **6**, 87–101.
83 B. L. Sater, First Nrel Conference on Theromophotovoltic Generation of Electricity, 1995, **321**, 165–176.
84 P. G. Borden, *Appl. Phys. Lett.*, 1979, **35**, 553.
85 D. M. Wilt, N. S. Fatemi, R. W. Hoffman, Jr., P. P. Jenkins, D. J. Brinker, D. Scheiman, Proceedings of the XIII Space Photovoltaic Research and Technology Conference (SPRAT XIII). NASA CP-3278, 440 pages, published by NASA, Washington, D.C, 1994, p. 341.
86 S. Wojtczuk, T. Parodos, G. Walker, Proceedings of the XIII Space Photovoltaic Research and Technology Conference (SPRAT XIII). NASA CP-3278, 440 pages, published by NASA, Washington, D.C., 1994, p. 363.
87 N. S. Fatemi, D. M. Wilt, P. P. Jenkins, R. W. Hoffman, V. G. Weizer, C. S. Murray and D. Riley, *Thermophotovoltaic Generation of Electricity*, 1997, **401**, 249–262.
88 N. S. Fatemi, D. M. Wilt, P. P. Jenkins, V. G. Weizer, R. W. Hoffman, C. S. Murray, D. Scheiman, D. Brinker and D. Riley, presented in part at the Photovoltaic Specialists Conference, Anaheim, CA, USA, Sep. 29–Oct. 03, 1997.
89 J. S. Ward, A. Duda, M. W. Wanlass, J. J. Carapella, X. Wu, R. J. Matson, T. J. Coutts, T. Moriarty, C. S. Murray and D. R. Riley, *Thermophotovoltaic Generation of Electricity*, 1997, **401**, 227–236.
90 N. S. Fatemi, D. M. Wilt, R. W. Hoffman, M. A. Stan, V. G. Weizer, P. P. Jenkins, O. S. Khan, C. S. Murray, D. Scheiman and D. Brinker, *Thermophotovoltaic Generation of Electricity*, 1999, **460**, 121–131.
91 W. David, W. Rebecca, P. Marc, W. Mark and M. Christopher, *Semicond. Sci. Technol.*, 2003, **18**, S209.
92 A. Krier, *Mid-infrared Semiconductor Optoelectronics*, Springer-Verlag, London, 2006.
93 R. A. Sinton, Y. Kwark, J. Y. Gan and R. M. Swanson, *IEEE Electron Device Lett.*, 1986, **7**, 567–569.
94 J. Y. Gan and R. M. Swanson, presented in part at the Photovoltaic Specialists Conference, Conference Record of the Twenty First IEEE, Kissimmee, FL, 21–25 May 1990.

 

95 A. E. Delahoy and A. M. Payne, presented in part at the Photovoltaic Specialists Conference, Conference Record of the Twenty Fifth IEEE, Washington, DC, 13–17 May 1996.
96 M. D. Archer and R. Hill, *Clean Electricity from Photovoltaics*, Imperial College Press, 2001.
97 M. W. Dashiell, J. E. Beausang, H. Ehsani, G. J. Nichols, D. M. Depoy, L. R. Danielson, P. Talamo, K. D. Rahner, E. J. Brown, S. R. Burger, P. M. Fourspring, W. E. Topper, P. F. Baldasaro, C. A. Wang, R. K. Huang, M. K. Connors, G. W. Turner, Z. A. Shellenbarger, G. Taylor, J. Z. Li, R. Martinelli, D. Donetski, S. Anikeev, G. L. Belenky and S. Luryi, *IEEE Trans. Electron Devices*, 2006, **53**, 2879–2891.
98 V. Khvostikov, N. Kalyuzhnyy, S. Mintairov, N. Potapovich, M. Shvarts, S. Sorokina, A. Luque and V. Andreev, *10th International Conference on Concentrator Photovoltaic Systems (Cpv-10)*, 2014, **1616**, pp. 21–24.
99 R. A. Sinton and R. M. Swanson, presented in part at the 19th IEEE Photovoltaic Specialists Conference, May 4–8, 1987.
100 J. Y. Gan, PhD thesis, Stanford University, 1990.
101 R. M. Swanson, presented in part at the proceeding of the 4th international photovoltaic science and engineering conference, Sydney 1989.
102 D. J. Friedman, A. J. Ptak, S. R. Kurtz, J. F. Geisz and J. Kiehl, presented in part at the International Conference on Solar Concentrators for the Generation of Electricity or Hydrogen, Scottsdale, Arizona 1–5 May 2005.
103 M. A. Green, *Solid-State Electron.*, 1981, **24**, 788–789.
104 M. A. Green, *Solar cells: operating principles*, Technology and system applications Prentice-Hall, Inc, Englewood Cliffs, NJ, 1992.
105 H. Kiess and W. Rehwald, *Sol. Energy Mater. Sol. Cells*, 1995, **38**, 45–55.
106 A. Lenert, D. M. Bierman, Y. Nam, W. R. Chan, I. Celanovic, M. Soljacic and E. N. Wang, *Nat. Nanotechnol.*, 2014, **9**, 126–130.
107 A. Vossier, F. Gualdi, A. Dollet, R. Ares and V. Aimez, *J. Appl. Phys.*, 2015, **117**, 015102.
108 M. A. Steiner, J. F. Geisz, I. García, D. J. Friedman, A. Duda and S. R. Kurtz, *J. Appl. Phys.*, 2013, **113**, 123109.
109 O. D. Miller, E. Yablonovitch and S. R. Kurtz, *IEEE J. Photovoltaics*, 2012, **2**, 303–311.
110 K. Tanabe, *Energies*, 2009, **2**, 504–530.
111 M. Yamaguchi, *Physica E*, 2002, **14**, 84–90.
112 M. Yamaguchi, T. Takamoto, K. Araki and N. Ekins-Daukes, *Sol. Energy*, 2005, **79**, 78–85.
113 I. Mathews, D. O'Mahony, B. Corbett and A. P. Morrison, *Opt. Express*, 2012, **20**(suppl 5), A754–A764.
114 F. J. Brooks, *GE Power Systems*, Schenectady, NY, 2000.
115 R. Kehlhofer, B. Rukes, F. Hannemann and F. Stirnimann, *Combined-cycle gas & steam turbine power plants*, PennWell Books, 2009.
116 F. DeAngelis, MSc thesis, Georgia Institute of Technology, 2016.